Impact of different types of planar defects on current transport in Indium Phosphide (InP)

Christian Dam Vedel[1,2,*], Enrico Brugnolotto[1,3], Søren Smidstrup[2], Vihar P. Georgiev[1]
Device Modelling Group, School of Engineering, University of Glasgow, Glasgow G12 8QQ, United Kingdom[1]
Synopsys Denmark ApS, Fruebjergvej 3, 2100 Copenhagen, Denmark[2]
IBM Research Europe-Zurich, 8803 Rüschlikon, Switzerland[3]
Correspondence author: christianvedel@hotmail.com[*]

***Abstract*—In this paper we show first-principles simulation results of the three most commonly occurring types of planar defects in Indium Phosphide (InP), which are Rotational Twin Planes (RTPs) and two types of Stacking Faults (SFs). We have found that only the two less common of these defects, the extrinsic and intrinsic SFs, have an impact on the current flow in the semiconductor. These two types of defects cause an increase in the resistivity of the semiconductor and a remarkable decrease in currents for low voltages. The most commonly occurring defect type, RTPs, were revealed to have little to no effect on the electrical properties of the semiconductor.**

***Index Terms*—Density Function Theory (DFT), First-principles simulation, Defects, III-V semiconductor, Indium Phosphide (InP)**

I. Introduction

III-V semiconductors, such as Indium Phosphide (InP) and its alloys, are widely researched due to their unique electrical and optical properties, such as high carrier mobilities [1], [2], direct and tunable band-gaps [3], [4] and low exciton binding energies [5], [6]. These properties can be exploited to improve on existing devices such as MOSFETs [7] and PIN photodiodes [8] or to pioneer novel new devices such as lasing microdisks [9] and topological photonics [10].
When growing III-V semiconductors with conventional growth methodologies, a large number of planar defects such as Stacking Faults (SFs) and Rotational Twin-Planes (RTPs) occur. Growth processes which mitigate and control the formation of these defects have been developed [11]–[14], as it has been experimentally validated that these defects degrade device performance. Specifically it was shown that RTPs reduce mobility, carrier lifetime and quantum efficiency in III-V nanowires [15]–[17]. Theoretical investigations have shown that twin-planes acts as scattering centres in Silicon [18], but also that in low densities, they have no effect on the current in InP nanowires [19]. The work reported here is an attempt to shine some more light on this complicated issue, using the state-of-the-art simulation software Synopsys QuantumATK [20]. Our aim is to calculate the resistance induced by the defects, as well as their impact on the current-voltage (I-V) characteristics of bulk InP for device usages.

This project has received funding from the European Union's Horizon 2020 research and innovation program under grant agreement No 860095 MSCA-ITN-EID DESIGN-EID.

II. Simulation Methodology

All calculations in this paper were performed using the atomistic first-principles simulation methodology called Density Functional Theory (DFT), wherein the electron density is treated as the fundamental variable [21]–[23]. Atoms are treated explicitly through basis sets consisting of Linear Combination of Atomic Orbitals (LCAO) and their corresponding pseudopotential. In this work the "High accuracy" version of the PseudoDojo set [24], as implemented in QuantumATK, were used. Exchange and correlation effects were approximated at the level of a Generalized Gradient Approximation (GGA), especially made for solids by Perdew, Burke and Emzerhof (PBES) [25]. To simulate current transport, DFT was combined with Non-Equilibrium Green Functions (NEGF), to accurately describe electrodes at finite bias [26]. The Brillouin zone were sampled with a k-point density of $300\,\text{Å}$ in the transport direction and $8\,\text{Å}$ in the transverse directions. The real space density mesh cutoff used were $85\,\text{Ha}$.
To construct the systems of interest, first bulk InP in the Zinc-Blende (ZB) phase were relaxed, until the forces between the atoms were no larger than $0.05\,\text{eV/Å}$. The resulting lattice constant of $5.890\,\text{Å}$ agrees well with the experimental value of $5.869\,\text{Å}$. The crystal were then cleaved along the $[1\,1\,1]$-direction, in which the crystal has an ABC stacking sequence of polarised layers, each layer having both a plane of Indium and Phosphor atoms. For the semi-infinite electrodes, three layers were used in order to repeat the stacking sequence. The finite central region were built with 38 layers, corresponding to $149\,\text{Å}$, to allow for any induced potential to be screened in the electrodes. The simple unit cell were $4.165\,\text{Å}$ wide in the transverse directions, and periodic boundary conditions were imposed to reproduce an infinite bulk. An n-type intrinsic background doping, corresponding to $1 \times 10^{17}\,\text{cm}^{-3}$, were added as compensation charges to all atoms in the system.

Six systems were inspected in total, a pristine InP system, as reference, and five defect systems with the defects located in the middle of the central regions. Both types of SF defects were considered, the extrinsic SF, where a layer is missing in the stacking sequence (ABC_BCA), and the intrinsic SF, where a layer is added (ABCBABC). Three RTP defect systems were also considered, one with a single RTP, one

with two RTPs seperated by 10 layers and finally two RTPs back-to-back.

In literature the two terms RTPs or simply ”twins” and SFs are often used interchangeably and referring to different kind of defects, sometimes even in different crystallographic phases. This necessitates a brief explanation of the terms used in the current work. In this work, a SF is when a layer is either removed or added to the $[1\,1\,1]$ ZB stacking sequence, but the sequence is otherwise uninterrupted and the added layer is identical to other layers in the crystal, (see Fig. 1b & 1c).
RTPs on the other hand is a type of twin-plane wherein the crystal is rotated $60°$ around the $[1\,1\,1]$-direction at the plane. The resulting crystal appears as a mirror-image with the atomic species swapped, (see Fig. 1a).
In a crystal where one species is much larger than the other, such as InP, two RTPs back-to-back is indistinguishable from an intrinsic SF, which explains the confusion of the terms in the literature. The stacking sequence of a ZB crystal in any $\langle 1\,1\,1\rangle$-direction can be investigated by HR-STEM images taken from the $\langle 1\,1\,0\rangle$-directions. Two such examples can be seen in Fig. 2, where in 2a the defects are clearly RTPs, since the stacking changes direction after the defect, but in 2b it is not clear whether the defect is an intrinsic SF or two RTPs.

III. Results and Discussion

To investigate the defects' perturbation of the system, the Hartree difference potential was projected onto the transport direction of the systems. The Hartree difference potential is the electrostatic potential of the electron density, calculated from the Poisson equation, except that the compensation charge density, from the added doping, is subtracted. There was a notable difference between the SFs and the RTPs potential, but only small variations between the different RTP systems, thus only one of each type is shown in Fig. 3. The rapid oscillations in the potential is the inter-atomic potential between subsequent atomic layers. To better visualise the perturbation of the potential, the envelope were also plotted. The perturbation from a single RTP, seen in Fig. 3a, is insubstantial compared to the periodic inter-atomic potential. In contrast the potential barrier caused by the extrinsic SF, seen in Fig. 3b, is large enough to severely hinder carrier transport.

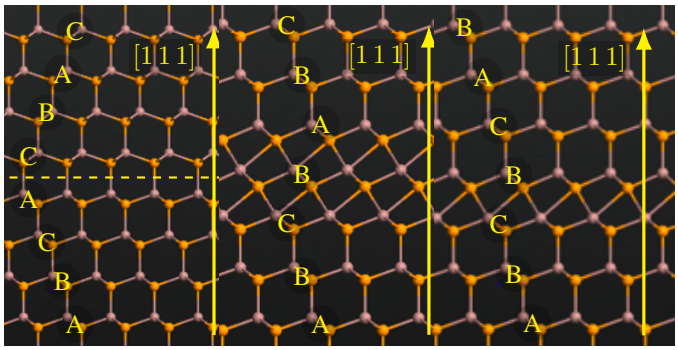

(a) A single RTP (b) Extrinsic SF (c) Intrinsic SF

Fig. 1. Three types of planar defects in a ZB InP crystal.

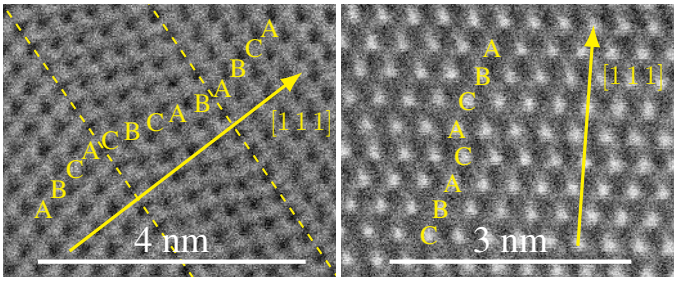

(a) Two RTPs separated by three layers (b) An intrinsic SF or two RTPs

Fig. 2. HR-STEM images of InP in the zinc-blende phase, seen from the $\langle 1\,1\,0\rangle$-direction, which allows vision of the stacking in the $\langle 1\,1\,1\rangle$-direction.

To quantify how much the potential barriers, caused by the defects, hinder current transport, a contact resistance was calculated.

$$R_{\text{contact}} = R_{\text{cent}} - R_{\text{elec}} = \frac{1}{G_{\text{cent}}} - \frac{1}{G_{\text{elec}}} \tag{1}$$

Where in (1) $R_{\text{cent(elec)}}$ and $G_{\text{cent(elec)}}$ is the resistance and conductance of the central (electrode) region respectively. The conductance is calculated in the usual fashion from the transmission spectrum:

$$G_{\text{cent}} = \int T_{\text{cent}}(E)\left(-\frac{\partial f(E)}{\partial E}\right) dE \tag{2}$$

where T_{cent} is the transmission spectrum and $f(E)$ is the Fermi-Dirac distribution. The contact resistance (1) was evaluated for all systems for various Fermi level shifts (i.e. doping

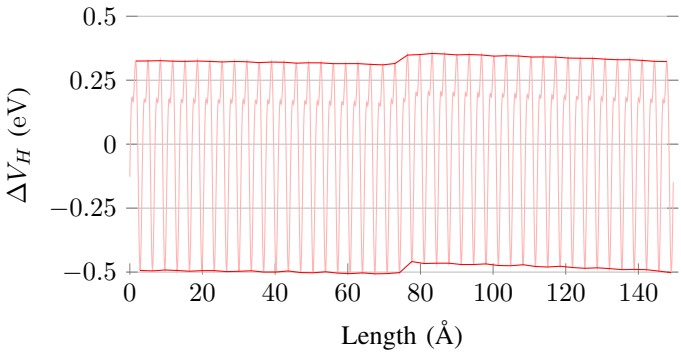

(a) A single twin-plane

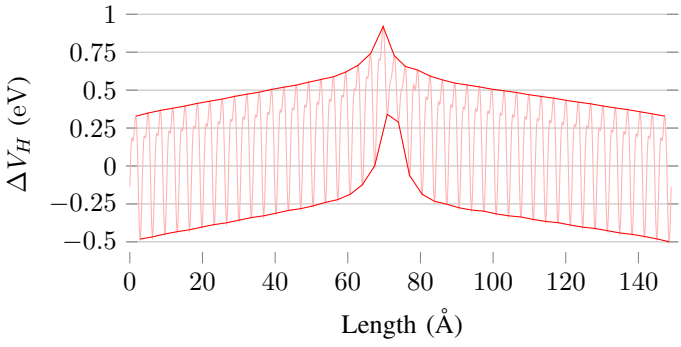

(b) Extrinsic SF

Fig. 3. Hartree difference potential, ΔV_H, along the transport direction. The potentials' envelopes are highlighted in solid red.

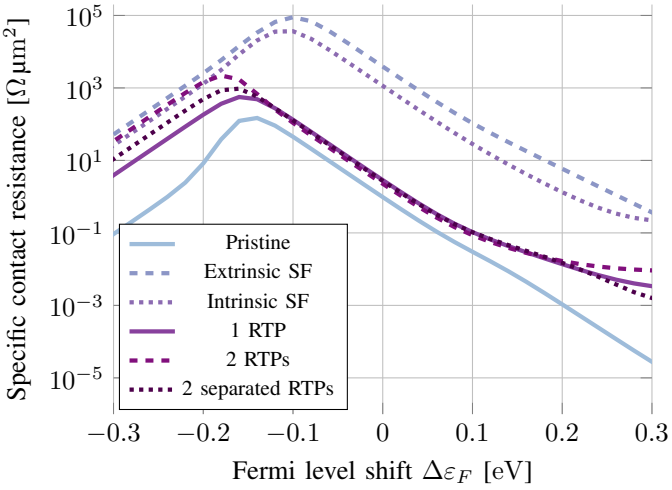

Fig. 4. Specific contact resistance of the five defects and a pristine reference system as a function of the Fermi level shift. $\Delta\varepsilon_F = 0\,\mathrm{eV}$ corresponds to the n-type intrinsic background doping of $1 \times 10^{17}\,\mathrm{cm}^{-3}$ and $\Delta\varepsilon_F = 0.17(-0.24)\,\mathrm{eV}$ corresponds to a n(p)-type doping of $6 \times 10^{19}\,\mathrm{cm}^{-3}$.

levels), the results are shown in Fig. 4. To interpret the shown results, it is worth mentioning that a high p-type doping of $6 \times 10^{19}\,\mathrm{cm}^{-3}$ corresponds to a Fermi shift of $-0.24\,\mathrm{eV}$ whereas a similar high n-type doping corresponds to a Fermi shift of $0.17\,\mathrm{eV}$. We find an increase in resistance across all defect systems as expected. Due to the large potential barrier from the SFs, the specific contact resistance is increased by four orders of magnitude for these systems, for intermediate doping levels, with the extrinsic SF having a four times higher resistance compared to the intrinsic SF. For the RTP systems on the other hand, the resistance is only increased three times compared to the pristine system for intermediate doping levels. Interestingly there is no further increase in the resistance from the additional RTP at these doping levels. At high doping levels the resistance increase from the RTPs rises, and especially for p-type doping we start to see a large effect in comparison to the pristine system. Notably at high p-type doping there is also a difference between the RTP systems, with the RTP system with two RTPs back-to-back having the larger increase in resistance.

To further investigate how much the defects perturb the current flow, I-V curves for the systems were calculated for a bias-range of $0\,\mathrm{V}$ to $1.3\,\mathrm{V}$, these can be seen in Fig. 6. Despite the triple resistance of the systems with RTPs as compared to the pristine InP, we do not see any noticeable difference in the current of these systems. All these systems shows app. constant current values until the breakdown voltage at app. $0.6\,\mathrm{V}$, after which they increase linearly on a log scale. The breakdown voltage at $0.6\,\mathrm{V}$ corresponds to the band gap achieved with the used simulation parameters.

It is well known that DFT is notorious for underestimating band gaps, but otherwise yields good results in agreement with experiments. While there does exist methods to achieve a better band gap, these methods are more computationally expensive and does not improve on any achieved results that are not directly related to the band gap. As this work is an investigation of electrical properties, these methods were not used and the value of the breakdown voltage should not be considered seriously. The current in the SF systems are strongly reduced, by several orders of magnitude even, for low voltages. As the voltage is increased, the potential barriers are slowly lowered compared to the conduction states, and the current approaches that of the pristine and RTP systems. The barrier still blocks out a few conduction states and as such the current does not actually reach the pristine and RTP systems. The intrinsic SFs current approaches the pristine system quicker than the extrinsic SF, which fits with it having a lower barrier to be overcome. Interestingly once it has been overcome, the intrinsic SFs barrier actually blocks out more conduction states than the extrinsic SF. Unfortunately despite great efforts and much time spent on it, it was not possible to converge the I-V curves for the SFs above app. $0.3\,\mathrm{V}$. We think that this is due to the induced potential barrier, shown in Fig. 3b, not being completely screened out in the electrodes. To visualise the conduction states and the SFs influence on these, the projected Local Density Of States (LDOS), projected along the transport direction, is plotted for all systems at zero bias, these are shown in Fig. 5. The conduction and valence band edges, marked by the yellow lines, are estimated automatically, and due to the slightly coarse sampling of the LDOS, artefacts appear as small sharp peaks that should be disregarded.

When comparing the LDOS of the pristine system in Fig. 5a with the RTP systems in Fig. 5d, 5e and 5f, we see that the RTPs barely disturbs the states of the systems. There is a slight relocation of high- and low-energy states and a few of the states in the conduction (valence) band disperses (congegrates) near the RTP, causing a small area at the RTP (next to the RTP) having less states for transport, which explains the three times increase in the resistance.

The SFs seen in Fig. 5c and 5b on the other hand shows a huge difference in the position of states. For the intrinsic SF, some of the conduction and valence band states are shifted upwards in energy, with the largest shift occurring at the SF. The upwards shift of valence band states effectively reduces the band gap, suggesting that breakdown voltage would have occurred at lower voltages than for the pristine system, had the I-V curve been converged to completion. The upward shift of the conduction band states, lowers the current for low voltages and explains the large increase in resistance calculated earlier. Interestingly we here see a big difference between the extrinsic and intrinsic SF, namely that for the extrinsic SF, several trap levels occur in the band gap. In fact the amount of trap levels and the gap between them almost makes the system metallic at the SF. The conduction band states are also shifted more in energy and further away from the SF as compared to the intrinsic SF, which explains the higher resistance of this SF.

To estimate the likelihood of the formation of the planar defects considered in this paper, we look at their formation energies relative to the pristine InP system shown in Table I. The SFs, which have large detrimental effect on the current transport of the semiconductor, luckily also has relatively high

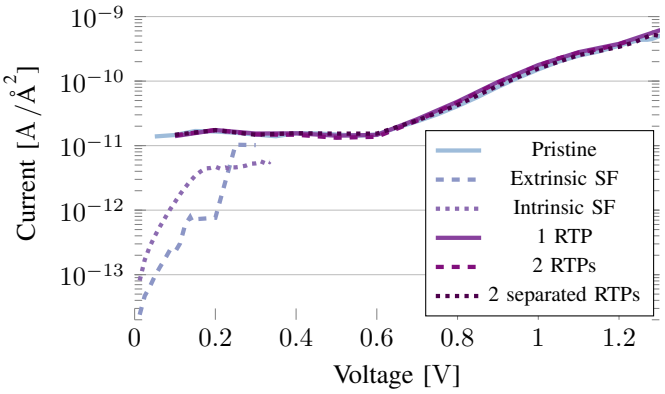

Fig. 6. I-V characteristic of the five defects and a pristine reference system.

formation energies, meaning that it is very unlikely that they will ever form. Especially the extrinsic SF, which was the more disruptive of the two, has a very high formation energy. In contrast the formation energy of the single RTP is so low, that it is very likely that it will form. In fact there seems to be a negative formation energy for the systems with two RTPs, suggesting that the true ground state of InP could be a twinning super-lattice. More investigation than was done in this paper, needs to be done for that result to be conclusive though. At the very least we can say that RTPs will be very hard to avoid forming, luckily as was shown in this paper, RTPs have almost no influence on current transport, at least at low densities. Yet more research needs to be done, to investigate the effect of high densities of RTPs on current transport, to conclude that RTPs are generally unimportant for electrical properties.

IV. Conclusion

In conclusion we have found that low densities of rotational twin-planes, have little to no effect on the current flow in undoped or lowly doped InP. Stacking faults of both the extrinsic and intrinsic kind, have a huge detrimental effect on current flow, but could perhaps be utilised in optical applications for their band gap narrowing effects. Their high formation energies mean that they will not occur naturally and great effort would be needed to fabricate them and as such optical applications seems unlikely.

V. Acknowledgment

We thank the operations team of the Binning and Rohrer Nanotechnology Center for their support. Results were obtained using the ARCHIE-WeSt High Performance Computer (www.archie-west.ac.uk) based at the University of Strathclyde.

TABLE I
Formation energies

System	Intrinsic SF	Extrinsic SF	1 RTP	2 RTPs	2 separated RTPs
Energy [eV]	0.5449	1.1820	0.0037	-0.2443	-0.2454

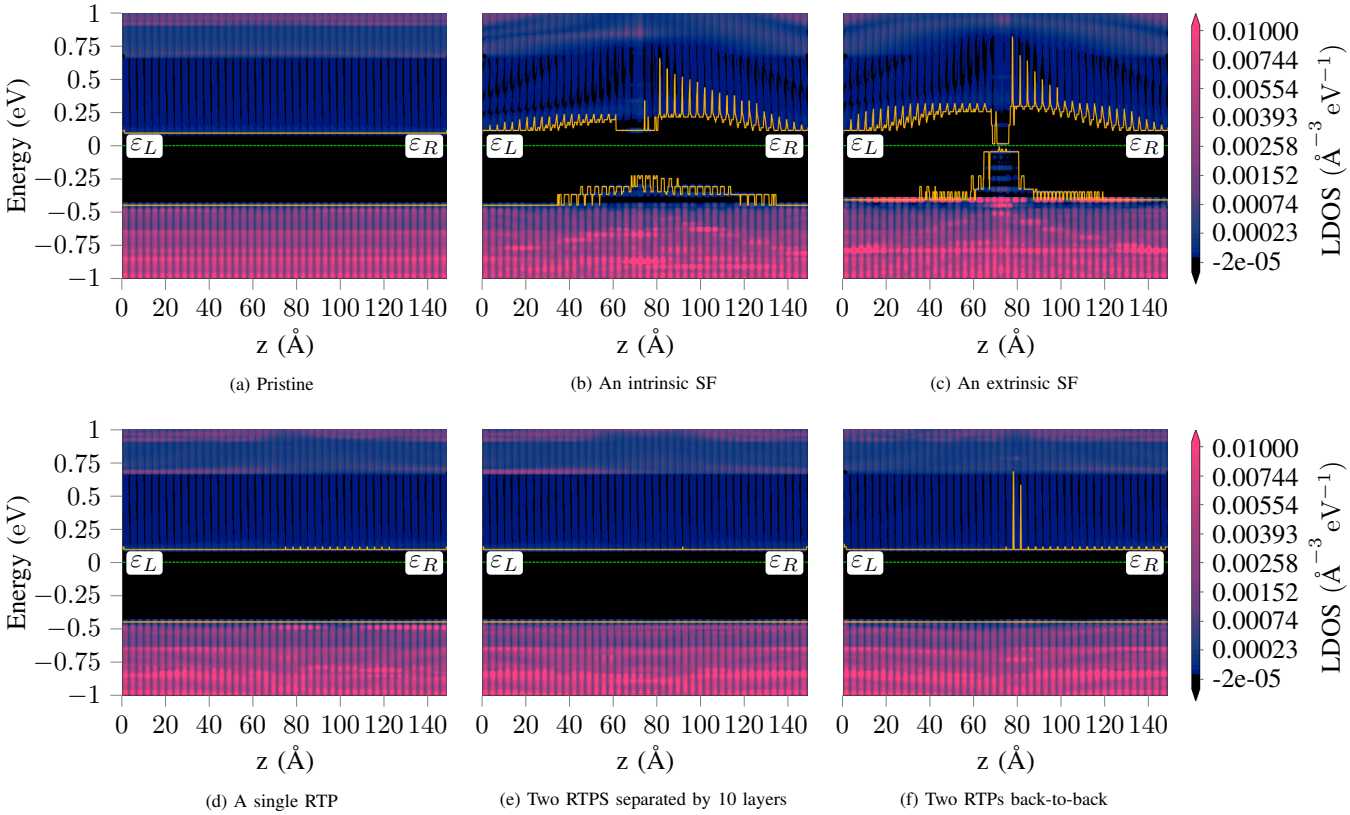

(a) Pristine (b) An intrinsic SF (c) An extrinsic SF

(d) A single RTP (e) Two RTPS separated by 10 layers (f) Two RTPs back-to-back

Fig. 5. Projected LDOS of calculated systems at zero bias. Conduction band minimum and valence band maximum is indicated by yellow lines.

References

[1] T. Skotnicki and F. Boeuf, "How can high mobility channel materials boost or degrade performance in advanced cmos," in *2010 Symposium on VLSI Technology*, 2010, pp. 153–154.

[2] P. Ong and L. Teugels, "5 - cmp processing of high mobility channel materials: Alternatives to si," in *Advances in Chemical Mechanical Planarization (CMP)*, S. Babu, Ed. Woodhead Publishing, 2016, pp. 119–135. [Online]. Available: https://www.sciencedirect.com/science/article/pii/B978008100165300005X

[3] I. Vurgaftman and J. R. Meyer, "Band parameters for nitrogen-containing semiconductors," *Journal of Applied Physics*, vol. 94, no. 6, pp. 3675–3696, 2003. [Online]. Available: https://doi.org/10.1063/1.1600519

[4] A. De and C. E. Pryor, "Predicted band structures of iii-v semiconductors in the wurtzite phase," *Phys. Rev. B*, vol. 81, p. 155210, Apr 2010. [Online]. Available: https://link.aps.org/doi/10.1103/PhysRevB.81.155210

[5] F. W. Wise, "Lead salt quantum dots: the limit of strong quantum confinement," *Accounts of Chemical Research*, vol. 33, no. 11, pp. 773–780, 2000, pMID: 11087314. [Online]. Available: https://doi.org/10.1021/ar970220q

[6] P. Reiss, M. Carrière, C. Lincheneau, L. Vaure, and S. Tamang, "Synthesis of semiconductor nanocrystals, focusing on nontoxic and earth-abundant materials," *Chemical Reviews*, vol. 116, no. 18, pp. 10 731–10 819, 2016, pMID: 27391095. [Online]. Available: https://doi.org/10.1021/acs.chemrev.6b00116

[7] C. Convertino, C. Zota, H. Schmid, D. Caimi, M. Sousa, K. Moselund, and L. Czornomaz, "Ingaas finfets directly integrated on silicon by selective growth in oxide cavities," *Materials*, vol. 12, no. 1, 2019. [Online]. Available: https://www.mdpi.com/1996-1944/12/1/87

[8] C. M. Oliver, K. E. Moselund, and V. P. Georgiev, "Evaluation of material profiles for iii-v nanowire photodetectors," in *21st International conference on Numerical Simulation of Optoelectronic Devices*, 2021, in press.

[9] P. Staudinger, S. Mauthe, N. V. Triviño, S. Reidt, K. E. Moselund, and H. Schmid, "Wurtzite InP microdisks: from epitaxy to room-temperature lasing," *Nanotechnology*, vol. 32, no. 7, p. 075605, nov 2020. [Online]. Available: https://doi.org/10.1088/1361-6528/abbb4e

[10] H. Zhao, P. Miao, M. H. Teimourpour, S. Malzard, R. El-Ganainy, H. Schomerus, and L. Feng, "Topological hybrid silicon microlasers," *Nature Communications*, vol. 9, no. 1, Mar 2018. [Online]. Available: http://dx.doi.org/10.1038/s41467-018-03434-2

[11] H. J. Joyce, Q. Gao, H. H. Tan, C. Jagadish, Y. Kim, X. Zhang, Y. Guo, and J. Zou, "Twin-free uniform epitaxial gaas nanowires grown by a two-temperature process," *Nano Letters*, vol. 7, no. 4, pp. 921–926, 2007, pMID: 17335270. [Online]. Available: https://doi.org/10.1021/nl062755v

[12] P. Staudinger, S. Mauthe, K. E. Moselund, and H. Schmid, "Concurrent zinc-blende and wurtzite film formation by selection of confined growth planes," *Nano Letters*, vol. 18, no. 12, pp. 7856–7862, 2018, pMID: 30427685. [Online]. Available: https://doi.org/10.1021/acs.nanolett.8b03632

[13] U. Krishnamachari, M. Borgstrom, B. J. Ohlsson, N. Panev, L. Samuelson, W. Seifert, M. W. Larsson, and L. R. Wallenberg, "Defect-free inp nanowires grown in [001] direction on inp (001)," *Applied Physics Letters*, vol. 85, no. 11, pp. 2077–2079, 2004. [Online]. Available: https://doi.org/10.1063/1.1784548

[14] R. E. Algra, M. A. Verheijen, M. T. Borgström, L.-F. Feiner, G. Immink, W. J. P. van Enckevort, E. Vlieg, and E. P. A. M. Bakkers, "Twinning superlattices in indium phosphide nanowires," *Nature*, vol. 456, pp. 369–372, 2008. [Online]. Available: https://doi.org/10.1038/nature07570

[15] P. Parkinson, H. J. Joyce, Q. Gao, H. H. Tan, X. Zhang, J. Zou, C. Jagadish, L. M. Herz, and M. B. Johnston, "Carrier lifetime and mobility enhancement in nearly defect-free core-shell nanowires measured using time-resolved terahertz spectroscopy," *Nano Letters*, vol. 9, no. 9, pp. 3349–3353, 2009, pMID: 19736975. [Online]. Available: https://doi.org/10.1021/nl9016336

[16] S. Perera, M. A. Fickenscher, H. E. Jackson, L. M. Smith, J. M. Yarrison-Rice, H. J. Joyce, Q. Gao, H. H. Tan, C. Jagadish, X. Zhang, and J. Zou, "Nearly intrinsic exciton lifetimes in single twin-free gaas/algaas core-shell nanowire heterostructures," *Applied Physics Letters*, vol. 93, no. 5, p. 053110, 2008. [Online]. Available: https://doi.org/10.1063/1.2967877

[17] R. L. Woo, R. Xiao, Y. Kobayashi, L. Gao, N. Goel, M. K. Hudait, T. E. Mallouk, and R. F. Hicks, "Effect of twinning on the photoluminescence and photoelectrochemical properties of indium phosphide nanowires grown on silicon (111)," *Nano Letters*, vol. 8, no. 12, pp. 4664–4669, 2008, pMID: 18983127. [Online]. Available: https://doi.org/10.1021/nl802433u

[18] M. D. Stiles and D. R. Hamann, "Electron transmission through silicon stacking faults," *Phys. Rev. B*, vol. 41, pp. 5280–5282, Mar 1990. [Online]. Available: https://link.aps.org/doi/10.1103/PhysRevB.41.5280

[19] C. Thelander, P. Caroff, S. Plissard, A. W. Dey, and K. A. Dick, "Effects of crystal phase mixing on the electrical properties of inas nanowires," *Nano Letters*, vol. 11, no. 6, pp. 2424–2429, 2011, pMID: 21528899. [Online]. Available: https://doi.org/10.1021/nl2008339

[20] S. Smidstrup, T. Markussen, P. Vancraeyveld, J. Wellendorff, J. Schneider, T. Gunst, B. Verstichel, D. Stradi, P. A. Khomyakov, U. G. Vej-Hansen, M.-E. Lee, S. T. Chill, F. Rasmussen, G. Penazzi, F. Corsetti, A. Ojanperä, K. Jensen, M. L. N. Palsgaard, U. Martinez, A. Blom, M. Brandbyge, and K. Stokbro, "Quantumatk: an integrated platform of electronic and atomic-scale modelling tools," *Journal of Physics: Condensed Matter*, vol. 32, no. 1, 2020. [Online]. Available: https://iopscience.iop.org/article/10.1088/1361-648X/ab4007

[21] P. Hohenberg and W. Kohn, "Inhomogeneous electron gas," *Phys. Rev.*, vol. 136, pp. B864–B871, Nov 1964. [Online]. Available: https://link.aps.org/doi/10.1103/PhysRev.136.B864

[22] W. Kohn and L. J. Sham, "Self-consistent equations including exchange and correlation effects," *Phys. Rev.*, vol. 140, pp. A1133–A1138, Nov 1965. [Online]. Available: https://link.aps.org/doi/10.1103/PhysRev.140.A1133

[23] S. Smidstrup, D. Stradi, J. Wellendorff, P. A. Khomyakov, U. G. Vej-Hansen, M.-E. Lee, T. Ghosh, E. Jónsson, H. Jónsson, and K. Stokbro, "First-principles green's-function method for surface calculations: A pseudopotential localized basis set approach," *Phys. Rev. B*, vol. 96, p. 195309, Nov 2017. [Online]. Available: https://link.aps.org/doi/10.1103/PhysRevB.96.195309

[24] M. Schlipf and F. Gygi, "Optimization algorithm for the generation of oncv pseudopotentials," *Computer Physics Communications*, vol. 196, pp. 36–44, 2015. [Online]. Available: https://www.sciencedirect.com/science/article/pii/S0010465515001897

[25] J. P. Perdew, A. Ruzsinszky, G. I. Csonka, O. A. Vydrov, G. E. Scuseria, L. A. Constantin, X. Zhou, and K. Burke, "Restoring the density-gradient expansion for exchange in solids and surfaces," *Phys. Rev. Lett.*, vol. 100, p. 136406, Apr 2008. [Online]. Available: https://link.aps.org/doi/10.1103/PhysRevLett.100.136406

[26] M. Brandbyge, J.-L. Mozos, P. Ordejón, J. Taylor, and K. Stokbro, "Density-functional method for nonequilibrium electron transport," *Phys. Rev. B*, vol. 65, p. 165401, Mar 2002. [Online]. Available: https://link.aps.org/doi/10.1103/PhysRevB.65.165401